CORROSION SCIENCE AND TECHNOLOGY, Vol.4, No.4(2005), pp.121~129

Design of Advanced Weathering Steel with High Corrosion Resistance for Structural Applications

B.K. Choi[1], H.G. Jung[2], J. Y. Yoo[2], and †K. Y. Kim[1]

[1]Pohang University of Science and Technology Center for Advanced Aerospace Materials San 31, Hyoja-Dong, Pohang 790-784 Korea
[2]POSCO Technical Research Labs., PO Box 36, Pohang 790-785 Korea

Basic design concept of the future steel structure requires environmental compatibility and maintenance free capability to minimize economic burdens. Recent trends in alloy design for advanced weathering steel include addition of various alloying elements which can enhance formation of stable and protective rust layer even in polluted urban and/or high Cl^- environment. The effects of Ca, Ni, W, and Mo addition on the corrosion property of Ca-modified weathering steel were evaluated through a series of electrochemical tests (pH measurement and electrochemical impedance spectroscopy: EIS) and structural analysis on rust layer formed on the steel surface.

Ca-containing inclusions of Ca-Al-Mn-O-S compound are formed if the amount of Ca addition is over 25 ppm. Steels with higher Ca content results in higher pH value for condensed water film formed on the steel surface, however, addition of Ni, W, and Mo does not affect pH value of the thin water film. The steels containing a high amount of Ca, Ni, W and Mo showed a dense and compact rust layer with enhanced amount of α-FeOOH. Addition of Ni, W and Mo in Ca-modified weathering steel shows anion-selectivity and contributes to lower the permeability of Cl^- ions. Effect of each alloying element on the formation of protective rust layer will be discussed in detail with respect to corrosion resistance.

Keywords *: weathering steel, Ca-modification, rust structure, pH measurement, EIS*

1. Introduction

Design concept of the future steel structure requires environmental compatibility and maintenance free capability. Most steel structures built with plain carbon steel need tremendous maintenance cost for painting to prevent surface corrosion. Painting the steel structure is not only continuous social economic burden but also great hazard to environment. To minimize such problems, weathering steel has been developed and used for limited applications. The weathering steel contains a small amount of Cu, P, Cr and/or Ni which enhance formation of a protective rust layer on the surface during a long-term exposure to the ambient atmosphere. This protective rust layer slows further corrosion, and thus it enables the weathering steel to be used for structural applications without painting.[1)] However, it takes a long time to develop the protective rust layer and the protective layer is difficult to be formed in the marine environment containing Cl^-. The final protective layer is known to be α-FeOOH layer which forms through phase transformation of γ-FeOOH and amorphous rust structure over decades. The α-FeOOH is thermodynamically the most stable rust phase and has a dense and compact structure and thus it suppresses penetration of the corrosive anions such as Cl^-.[2)-4)]

Current research efforts of alloy design for advanced weathering steel are focused mainly on the formation of a dense and stable rust layer even in high Cl^- environments. Major advancements include 1) addition of 5% Ni for formation of a dense and tight rust,[1)] 2) addition of Ni-Mo-P for formation of MoO_4^{2-} and PO_4^{2-} ions which prevent permeation of Cl^- ions through the rust layer,[2)] and 3) addition of Ca for formation of stable α-FeOOH in the alkali condition of the steel surface.[3)-5)] The beneficial effect of Ca addition on the corrosion properties of weathering steel is now reasonably well understood due to a series of investigations including theoretical estimation of the optimum range of Ca content in steel.[3)-5)] The main role of Ca with respect to corrosion properties is the formation of complex inclusions containing CaO and CaS, which can dissolve significantly in thin water film condensed on the steel surface. Dissolution of complex

†Corresponding author: kykim@postech.ac.kr

inclusions containing CaO and CaS increases the alkalinity of thin water film, which enhances the formation of a dense and protective α-FeOOH in the rust.

To maximize further the beneficial effect of Ca-modification of weathering steel, the role of a number of alloying elements of Ni, Mo, and W in rust formation is also required to determine the optimum composition of advanced weathering steel. In this paper, the effects of various alloying elements on the corrosion properties of advanced weathering steel are reviewed with respect to the electrochemical and structural aspects of rust layers.

2. Experimental

The chemical composition of the steel specimens used in this investigation is listed in Table 1. The inclusion present in the steel was analyzed to verify the existence of Ca-compound. To measure the pH value of water film on the steel, an ultra fine pH electrode was employed. Distilled water, 0.01 M and 0.1 M NaCl solution were used as the water film. EIS was performed in 0.01 M and 0.1M NaCl solutions using a two-electrode cell configuration. EIS was measured using a Frequency Response Detector coupled to a potentiostat in a frequency range of 10 kHz to 10 mHz with an amplitude of 10 mV. Cyclic corrosion tests were carried out in a corrosion chamber, which could simulate a marine environment with various conditions of wet and dry cycles and a Cl^- deposition rate of 0.8 mdd ($mg/dm^2/day$). After cyclic corrosion test, analysis of the rust layer included examination of rust morphology using scanning microscopy, and phase identification using Raman spectroscopy and Mössbauer spectroscopy.

Since corrosion resistance of weathering steel in sea environments greatly depends upon Cl^- ion permeability through rust layer, Cl^- ion permeability was evaluated by measuring the liquid-junction potential set up by the difference in KCl concentration between the two different compartments separated by the rust layer which serves as a permeable membrane. The liquid junction potential was measured in the KCl concentration range of 10^{-3} to 10^{-1}M for rust membranes prepared by cyclic corrosion test. Detailed information about experimental procedures used in this investigation including ingot preparation, inclusion analysis, pH measurement, EIS, cyclic corrosion test, and rust layer characterization can be found elsewhere.[5),7)]

3. Result and discussion

3.1 Analysis of inclusions

Addition of a small amount of Ca results in formation of calcium oxide or calcium sulfide. These oxide and sulfide usually form complex inclusions of Ca-Al-Mn-O-S during the steel making process. Fig. 1 shows a typical morphology and an elemental analysis of Ca-containing inclusion formed in N1 specimen containing 26 ppmCa-1%Ni. The complex inclusions had a round shape with diameters from 1-5 μm. Total amount of Ca determines critically the ratios of CaO to Al_2O_3 and of CaS to MnS in the inclusion. The ratios of CaO to Al_2O_3 and of CaS to MnS are greater than 1 with 26 ppmCa, but lower than 1 with 11 ppmCa.[7)] Alloying elements of Ni, W and Mo

Table 1. Chemical composition of tested specimens (wt%)

	C	Si	Mn	P	S	Cu	Al	Ni	W	Mo	Ca (ppm)
C1	0.145	0.402	1.53	0.016	0.006	-	0.028	-	-	-	-
C2	0.081	0.426	1.43	0.016	0.006	0.320	0.029	-	-	-	15
C3	0.083	0.465	1.40	0.014	0.010	0.312	0.034	0.992	-	-	40
SI1	0.107	0.226	1.06	0.015	0.009	0.430	0.049	1.03	-	-	60
SI2	0.099	0.385	0.98	0.013	0.010	0.395	0.038	0.97	-	-	64
SI3	0.107	0.620	0.99	0.013	0.010	0.401	0.039	0.99	-	-	68
N1	0.079	0.392	1.40	0.015	0.005	0.299	0.035	0.98	-	-	26
N2	0.082	0.403	1.40	0.012	0.006	0.302	0.034	1.48			27
N3	0.080	0.403	1.40	0.009	0.006	0.303	0.036	1.97	-	-	29
W1	0.079	0.398	1.40	0.013	0.006	0.298	0.031	0.98	0.198	-	26
W2	0.081	0.425	1.40	0.016	0.005	0.305	0.033	0.98	0.386	-	29
M1	0.086	0.378	1.42	0.015	0.006	0.302	0.034	0.99	-	0.200	29
M2	0.081	0.385	1.40	0.013	0.006	0.310	0.031	0.99	-	0.392	23

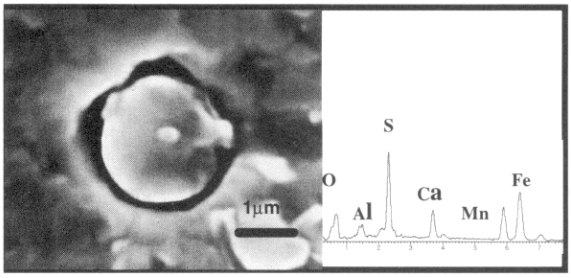

(a)

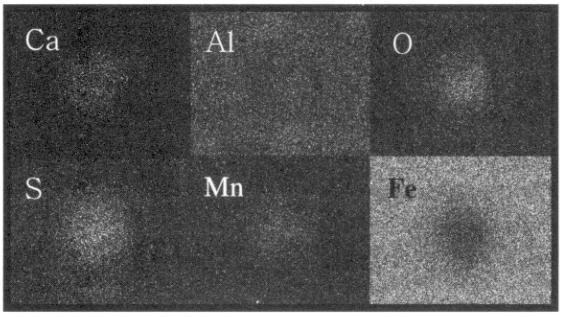

(b)

Fig. 1. (a) Inclusion morphology and EDS data of specimen N1, (b) Element mapping of inclusion formed in specimen N1

were not detected in the inclusions by EDS analysis. This means that addition of Ni, W and Mo does not affect the shape and composition of the inclusions.

3.2 pH Measurement

Fig. 2 shows the trend of pH change in thin water films covered on Ca-modified weathering steels containing various amounts of Ca, Ni, W, and Mo. Fig. 2(a) shows pH changes in distilled water film for specimens of C1, C2, C3, and N1 for which the amount of Ca is different. Specimens containing Ca less than 15 ppm show pH decreases over time, while those containing Ca higher than 26 ppm show pH increases with time up to 60 min. and then slowly decrease with time. However, pH change is not very sensitive to other alloying elements of Ni, W and Mo as well as their content. Figs. 2(b) and 2(c) show pH changes with time in 0.01 M and 0.1 M NaCl solutions. Comparing to the trend of pH changes in distilled water film, for the given specimens, pH values measured in NaCl solutions are generally lower, and decrease more in 0.1 M NaCl solution than in 0.01 M NaCl solution. For specimens containing Ca higher than 26 ppm, regardless of the kind and amount of alloying elements, the time for initial increase in pH value decreased more with higher Cl^- ion content. The decreasing rate of pH value after peak value was more rapid with higher Cl^- ion content. The pH values of specimens containing Ca less than 15 ppm ever decreased with time, and the decreasing rate was more rapid with higher Cl^- ion content. The decreasing trend of pH value may be due to hydrolysis of Fe^{2+} in the Cl^- ion containing solution since the thin water film is acidified by formation of free acid. It was also observed previously that that the presence of Si in Ca-modified weathering steel did not have a particularly adverse effect on pH value. These observations were consistent with the result of inclusion analysis from which inclusions containing Si could be hardly formed even in specimens containing 0.62% Si.[7]

3.3 Electrochemical impedance spectroscopy

An EIS test was performed to evaluate the short-term effect of various alloying elements on the corrosion resistance of weathering steel covered with a thin water film. Fig. 3 shows typical raw EIS data, which were measured for N1 and W2 specimens in 0.01 M NaCl solu-

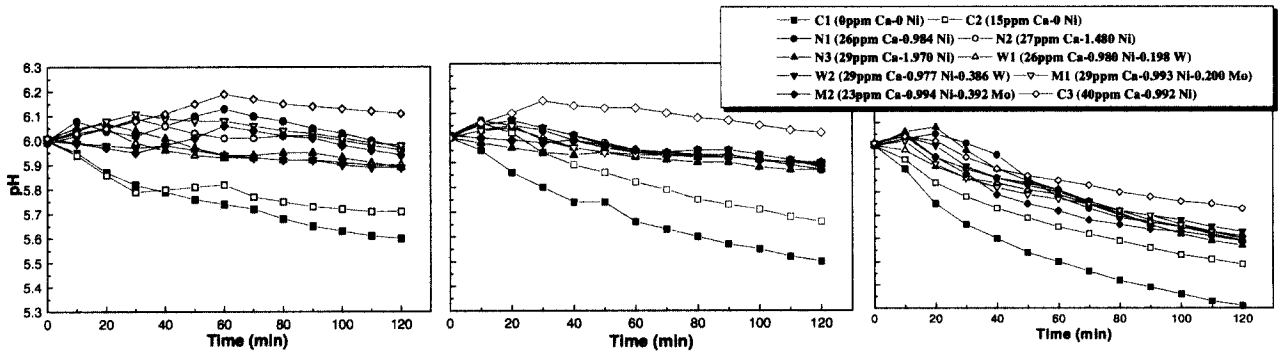

(a) (b) (c)

Fig. 2. Change in pH value of thin water film measured for 2 hours at room temperature using a micro-pH electrode; (a) in distilled water, (b) in 0.01M NaCl solution and (c) in 0.1M NaCl

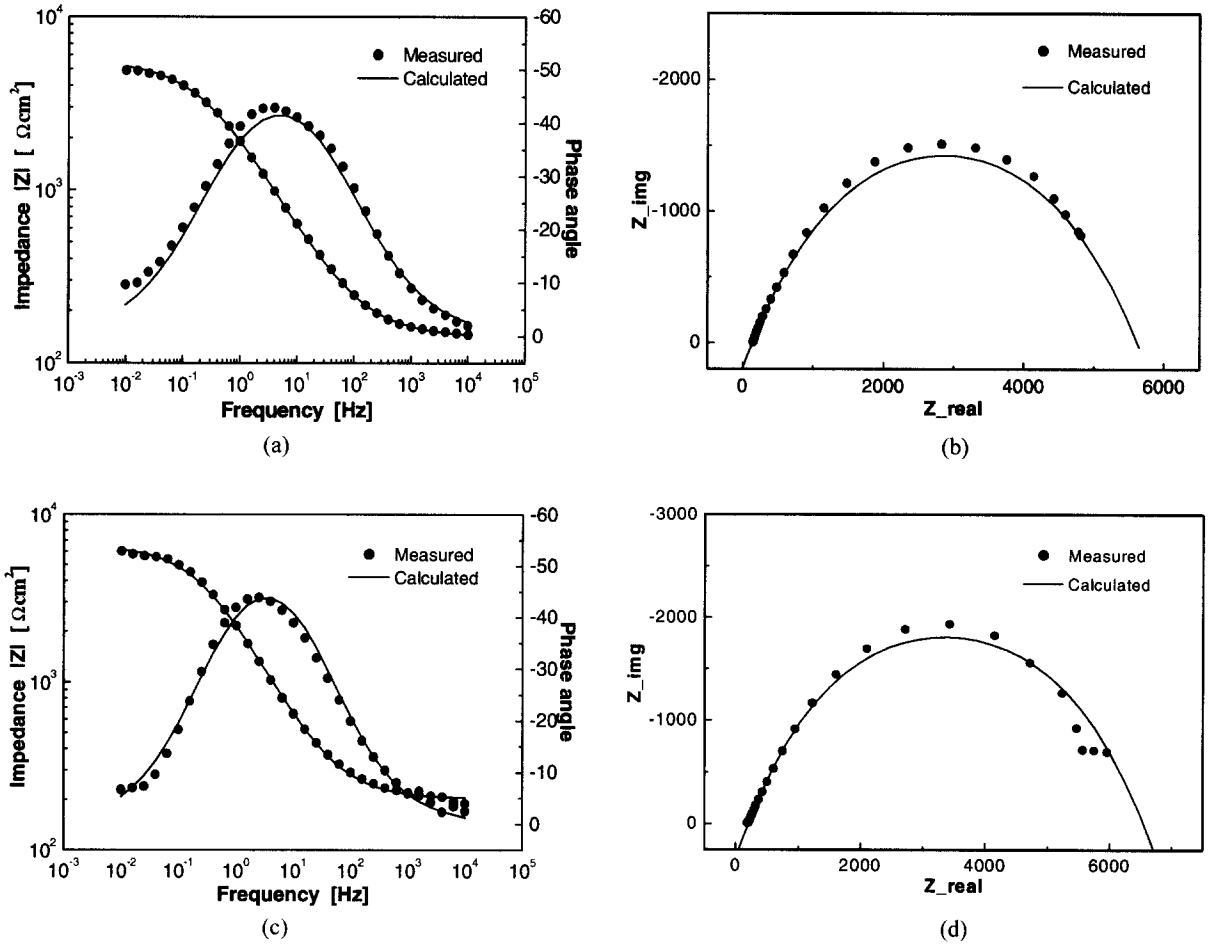

Fig. 3. Simulation for EIS data measured with a thin water film of 0.01M NaCl solution on the specimen surface; (a) and (b) for N1, and (c) and (d) for W2. Bode plot and Phage angle are shown in (a) and (c), while Nyquist plot is shown in (b) and (d)

Table 2. EIS parameters determined from a simulation program

No.	0.01 M NaCl				0.1 M NaCl			
	Rs (Ω-cm^2)	CPE ($S\sqrt{sec}\cdot cm^2$)	Frequency Power	Rp (Ω-cm^2)	Rs (Ω-cm^2)	CPE ($S\sqrt{sec}\cdot cm^2$)	Frequency Power	Rp (Ω-cm^2)
C1	161	3.2×10^{-4}	0.8	1.4×10^{3}	19	5.2×10^{-4}	0.8	1.3×10^{3}
C3	139	2.1×10^{-4}	0.8	3.3×10^{3}	19	3.3×10^{-4}	0.8	1.6×10^{3}
SI1	51	1.7×10^{-4}	0.8	8.9×10^{3}	13	13.4×10^{-4}	0.8	1.5×10^{3}
SI2	74	1.3×10^{-4}	0.8	8.0×10^{3}	4	6.0×10^{-4}	0.8	1.4×10^{3}
SI3	73	4.0×10^{-4}	0.8	1.7×10^{3}	5	9.6×10^{-4}	0.8	1.2×10^{3}
N1	141	1.4×10^{-4}	0.8	5.5×10^{3}	19	3.0×10^{-4}	0.8	1.6×10^{3}
N3	135	1.2×10^{-4}	0.8	6.3×10^{3}	19	3.1×10^{-4}	0.8	3.3×10^{3}
W2	202	1.2×10^{-4}	0.8	6.3×10^{3}	14	1.8×10^{-4}	0.8	3.9×10^{3}
M2	145	1.4×10^{-4}	0.8	6.2×10^{3}	16	2.9×10^{-4}	0.8	3.4×10^{3}

tion, in the form of Nyquist and Bode plots superimposed with best curve fits calculated by an EIS software. Since the phase angle for all the specimens exceeds -45° on the Bode plot, corrosion of the specimens can be considered to occur uniformly and thus a simple Randle circuit can be adopted to analyze all EIS data.

Table 2 lists the values of R_s, CPE, R_p, and Frequency Power (FP) factor for all specimens tested in 0.01 M and

0.1 M NaCl solutions.

In general, although there are some scatterings in the determined values, their values are within a reasonable range of physical parameters. For solution resistance, R_s values of 0.01 M NaCl solutions vary from 135-202 Ω-cm^2 with an average value of 154 Ω-cm^2, while those of 0.1 M NaCl solutions vary from 14-19 Ω-cm^2 with an average value of 18 Ω-cm^2. There is nearly one order of difference between the solution resistances of the 0.01 M and 0.1 M NaCl solutions. In 0.01 M NaCl solution, the R_p value increases as Ca content increases (C1 vs. C2), and it further increases as the alloying elements of Ni, W, and Mo are added (N1, N3, W2, M2). High R_p value is an indication of high corrosion resistance. It is interesting to note that the R_p values of W2 and M2, which contain only 0.4%W and 0.4%Mo in addition to 1%Ni, respectively, are higher than those of N3 which contains 2%Ni. It has an industrial significance for alloy design of the weathering steel since design of a lower cost weathering steel with higher corrosion resistance can be possible with addition of only 0.4%Mo or 0.4%W instead of increasing the high cost Ni content to 2% or even higher. A similar effect of alloying elements on the R_p value can also be observed from the EIS data analyzed for 0.1M solution.

3.4 Cyclic corrosion test simulating a marine environment

In order to understand the effect of the kind and amount of various alloying elements on the structure and phase of a rust layer, corrosion tests were performed in a cyclic

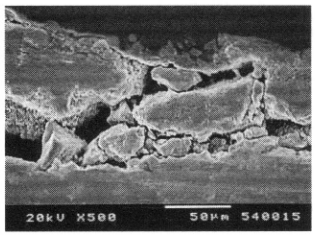

(a) Specimen C1 (0ppm Ca)

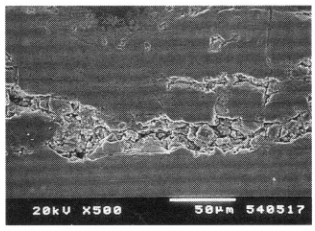

(b) Specimen C3 (40ppm Ca-0.99 Ni)

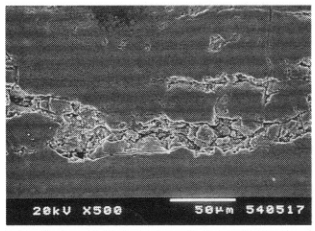

(c) Specimen N1 (0.98 Ni)

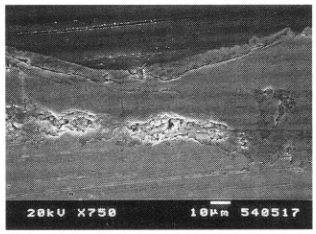

(d) Specimen N3 (1.97 Ni)

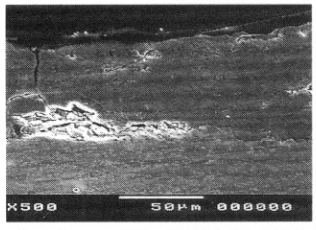

(e) Specimen W1 (0.98 Ni-0.20 W)

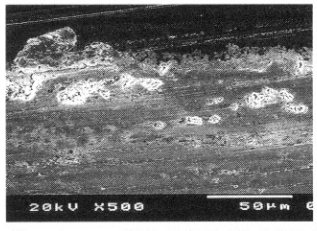

(f) Specimen W2 (0.98 Ni-0.39 W)

(g) Specimen M1 (0.99 Ni-0.20 Mo)

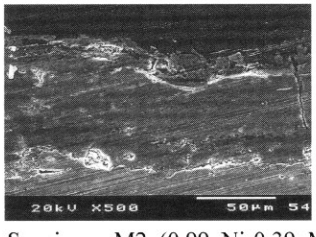

(h) Specimen M2 (0.99 Ni-0.39 Mo)

Fig. 4. Cross-sectional morphology of rust layers formed on weathering steel after cyclic corrosion tests (480 cycles)

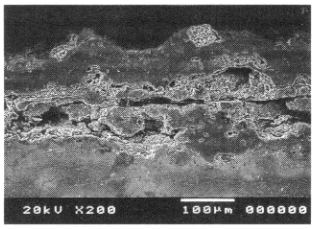

(a) Specimen C1 (0ppm Ca)

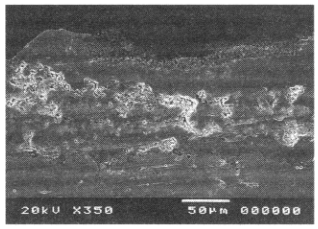

(b) Specimen C3 (40ppm Ca-0.99 Ni)

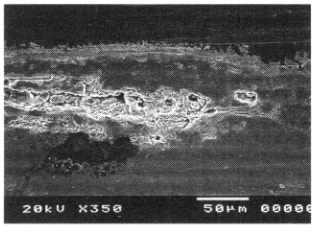

(c) Specimen N1 (0.98 Ni)

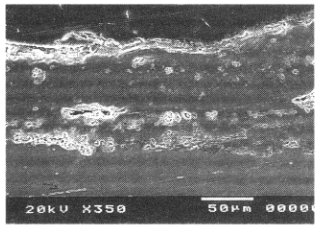

(d) Specimen N3 (1.97 Ni)

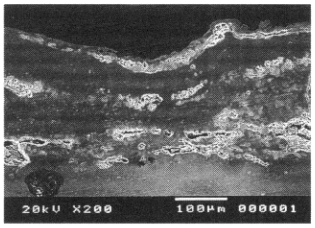

(e) Specimen W1 (0.98 Ni-0.20 W)

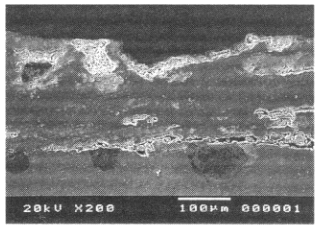

(f) Specimen W2 (0.98 Ni-0.39 W)

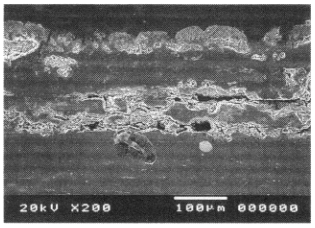

(g) Specimen M1 (0.99 Ni-0.20 Mo)

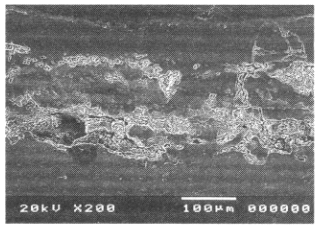

(h) Specimen M2 (0.99 Ni-0.39 Mo)

Fig. 5. Cross-sectional morphology of rust layers formed on weathering steel after cyclic corrosion tests (720 cycles)

corrosion chamber simulating a marine environment under cyclical wet and dry conditions. Although both pH measurement and EIS tests provide valuable information about the chemical and electrochemical nature of steel specimens exposed to aqueous environments within a reasonably short time period, they are not adequate for complete understanding of the corrosion properties of steel specimens, since the corrosion process is highly dependent upon the rust structure which forms on the surface of the steel. In order to evaluate the corrosion properties of weathering steel, understanding of the rust structure and its stability is particularly important.

Figs. 4 and 5 compare the cross-sectional morphologies of the rust layer which formed on the steel surface after 480 and 720 cycles, respectively. The cracks in the rust or crevices at the interface between the rust and substrate steel occurred due to mechanical stress applied by cutting and/or polishing during sample preparation, but not by corrosion process. In general, it was observed that the rust structure became dense and compact as the number of corrosion cycles and amount of the alloying elements of Ca, Ni, W, and Mo were increased. The number of cracks and crevices observed in the rust is an indirect indication of the compactness and stability of the rust since the number of those cracks and crevices became less for specimens with higher corrosion cycles and/or with higher amount of alloying elements.

In order to examine the effect of alloying elements on the compactness of the rust layer, the hardness of the rust layer was measured after 720 cycles, and the results are listed in Table 3. The hardness value increased as the content of Ca, Ni, W and Mo was increased. These results

strongly indicate that the corrosion resistance of Ca-modified steel can be improved with the addition of an optimum amount of Si, W and Mo by forming rust layers with compact structures. Comparison of hardness values of C1, C2, and C3 indicates that addition of 1%Ni refines the rust structure more in addition to the beneficial effect of Ca modification. Comparison between the hardness values of C3 and N1, both specimens having the same amount of 1%Ni, suggests that the beneficial effect of Ca may be obtained with Ca content at least higher than 40 ppm. With Ca content in the range of 23 to 29 ppm which is a recommended optimum range for commercial weathering steel, exceptionally high hardness can be obtained by addition of 0.4%W or 0.4%Mo.

Table 3. Hardness values of rust layers formed on steel specimens after cyclic corrosion tests (720 cycles)

Specimen	Hardness	Specimen	Hardness
C1 (0ppm Ca)	289	N3 (29ppm Ca-1.97 Ni)	407
C2 (15ppm Ca)	313	W1 (26ppm Ca-0.98 Ni-0.20 W)	403
C3 (40ppm Ca-0.99 Ni)	473	W2 (29ppm Ca-0.98 Ni-0.39 W)	511
N1 (26ppm Ca-0.98 Ni)	353	M1 (29ppm Ca-0.99 Ni-0.20 Mo)	438
N2 (27ppm Ca-1.48 Ni)	364	M2 (23ppm Ca-0.99 Ni-0.39 Mo)	442

Raman spectroscopy was employed to analyze phases consisting of rust layer. Fig. 6 shows the result of Raman spectroscopic analysis on rust layer formed on N1 (1%Ni-26ppmCa) after 720 cycles. This rust layer composed of a dark brown inner layer and bright orange-colored outer layer. It was identified that γ-FeOOH and Fe_3O_4 were present in both layers, but that α-FeOOH was mainly in the inner layer and β-FeOOH mainly in the outer layer. Since the amount of minor elements in weathering steel is below the critical detection limit of Raman spectroscopy and the main metallic element in the rust layer is Fe, it is clear that α-FeOOH is responsible for the compact structure of the inner rust layer.

Raman spectroscopy provides only qualitative information about the phases present in the rust layer. However, Mössbauer spectroscopy can be used to analyze quantitatively the fraction of the phases consisting of rust. Table

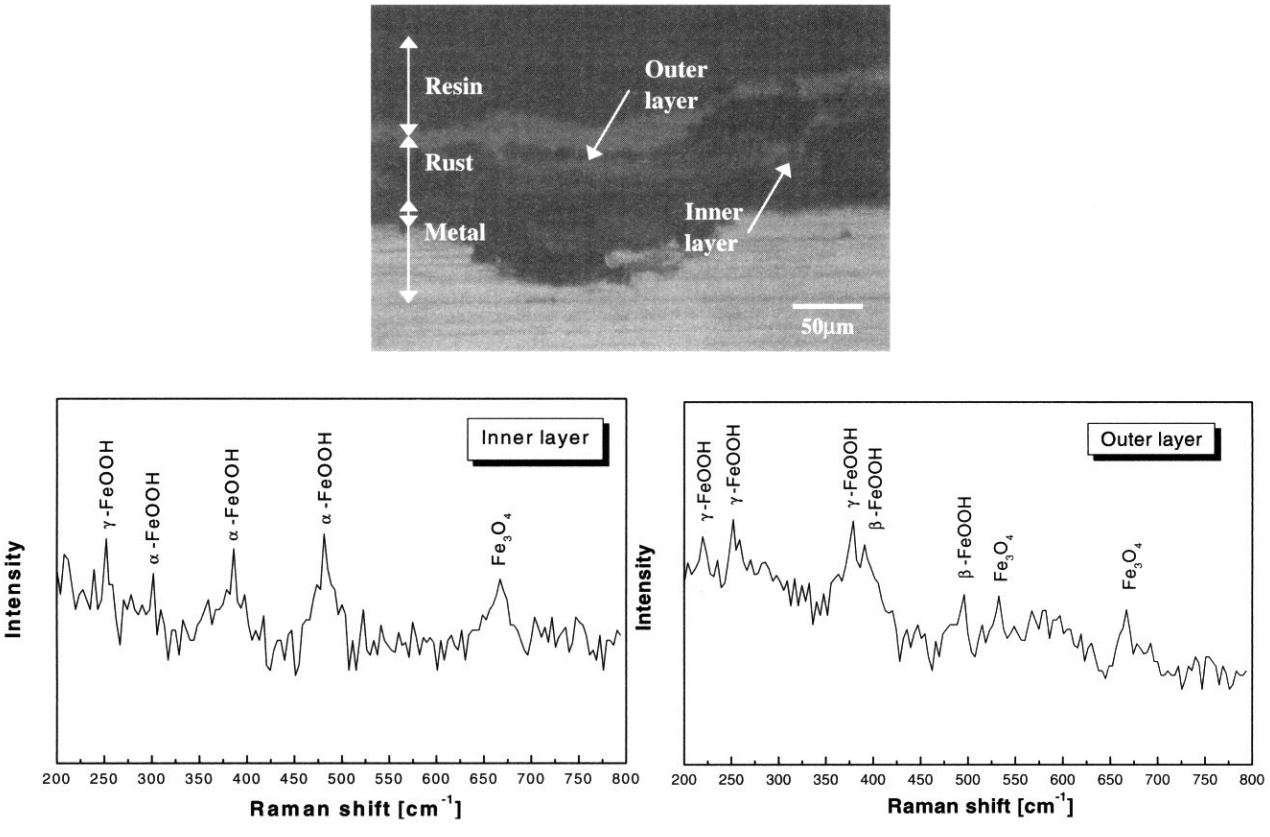

Fig. 6. Raman spectra of rust layers formed on N1 specimen corroded during 720 cycles

Table 4. Result of Mossbauer spectroscopic analysis on corrosion products obtained after 480 and 720 cycles

Corrosion products	480 cycles				720 cycles			
	N1	N3	W2	M2	N1	N3	W2	M2
α-FeOOH	12	15	22	18	13	18	33	20
β-+γ-FeOOH	15	12	11	20	9	9	13	20
Fe_3O_4	73	73	67	62	78	73	54	61

4 compares the fraction of phases present in the rust formed after 480 and 720 cycles. In general, a relatively high fraction of α-FeOOH is observed from specimens with higher Ni content (N1: 1%Ni vs. N3: 2%Ni) and with additional alloying elements of W (W2: 0.4%W) and Mo (M2: 0.4%No). Although specimens of N1, W2 and M2 have the same amount of 1%Ni and similar range of Ca content, a significantly high fraction of α-FeOOH is observed from both W2 and M2. The fractions of α -FeOOH of both W2 and M2 are even higher than those of N3 which contains 2%Ni. This means that addition of only 0.4%W or 0.4%Mo can greatly promote formation of protective α-FeOOH in rust, and such effect of W and Mo is better than that of Ni. As the corrosion cycles increased from 480 cycles to 720 cycles, the fraction of α-FeOOH increased relatively small amount. However, W2 specimen showed a significant increase from 22% to 33%.

This suggests that addition of a small amount of W, comparing with Ni and Mo, can provide better conditions for formation of protective α-FeOOH phase during long term exposure of weathering steel in a Cl^- ion-containing environment. An extremely high fraction of Fe_3O_4 is present in the rust of all the specimens. The Raman spectroscopy data showed previously that Fe_3O_4 is present in both inner and outer layers, and thus it is not clear whether Fe_3O_4 is present mainly in inner or outer layer.

Since two rust phases of γ-FeOOH and Fe_3O_4 can be formed from each other depending on the oxygen supply and solution chemistry.[8] When steel corrodes under a water film with a limited supply of oxygen, Fe_3O_4 can form by a γ-FeOOH reduction reaction.

$$8\ \gamma\text{-FeOOH} + Fe^{2+} + 2e^- \longrightarrow 3\ Fe_3O_4 + 4H_2O$$

If the water film is thin enough, the oxygen in the atmosphere can oxidize the Fe_3O_4 to form γ-FeOOH.

$$3\ Fe_3O_4 + 0.75O_2 + 4.5H_2O \longrightarrow 9\ \gamma\text{-FeOOH}$$

Therefore, it is clear that Fe_3O_4 is always present along with γ-FeOOH. According to the corrosion resistance evaluated by cyclic corrosion data, the corrosion resistance is not closely related with the fraction of Fe_3O_4, but rather with the fraction of α-FeOOH. This suggests that Fe_3O_4 does not make a continuous rust film, but forms isolated island type crystals mixed with γ-FeOOH. Thus, it seems that a high fraction of Fe_3O_4 does not directly contribute to the corrosion resistance of weathering steel although the crystal structure of Fe_3O_4 itself is dense and compact. However, a more careful examination on Fe_3O_4 crystals and their correlationship with corrosion rates should be investigated.

3.5 Permeability of Cl^--ion through the rust film

Corrosion resistance of weathering steel in sea environments depends upon Cl^- ion permeability through rust layers. Cl^--ion permeability can be evaluated by measuring the liquid-junction potential set up by the difference in Cl^- ion concentration between the two different compartments separated by a rust layer which serves as a permeable membrane. Fig. 7 shows the liquid junction potential measured for the rust membranes prepared by cyclic corrosion test. All the liquid junction potentials have positive slopes, and this means that the rust layers are permeable to the Cl^- ions (i.e., $t_- > 0.5$). The greater the value of positive slope is, the easier Cl^- ions can be permeable to the rust layer.

Although the slopes of the junction potential are not a clearly straight line, the permeability of Cl^- ions through the rust membrane can be qualitatively interpreted by grouping them by three; the most easily permeable ones for C2 and N1, the most difficult ones for C3 and W2, and the others having medium permeability. These junction potential data also support that the corrosion resistance can be enhanced by Ca-modification with Ca content greater than 40 ppm and by addition of a small amount of alloying elements of W or Mo in addition to

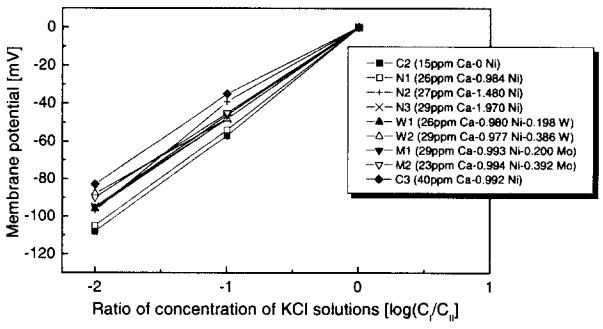

Fig. 7. Liquid-junction potentials measured for various rust membranes formed by cyclic corrosion tests

1%Ni. The Cl^- ion permeability data evaluated by measuring the junction potential are in good agreement with other test data of pH measurement, EIS, and cyclic corrosion tests.

4. Conclusions

Ca-modified steels form Ca-Al-Mn-O-S type inclusions if the amount of Ca addition is over 25 ppm. The steels containing high amount of Ca show increasing trend in pH value, while the steels with no Ca show decreasing trend in pH value. However, the effect of Ni, W and Mo addition on pH value is not significant. In EIS test, the steels containing higher amount of Ca, Ni, W and Mo show better corrosion resistance during initial stage of corrosion. The steels containing high amount of Ca, Ni, W and Mo show a dense and compact rust layer with enhanced α-FeOOH formation. The anion-selectivity of rust membrane is suppressed by addition of Ni, W and Mo in Ca-modified weathering steel.

References

1. A.Usami, *CAMP-ISIJ*, **9**, 482 (1996).
2. M. Yamashita H. Miyuki, Y. Matsuda, H. Naqano, and T. Misawa, *Corrosion Science*, **36**, 283 (1994).
3. M. Yamamoto, H. Kihira, A. Usami, K. Tanabe, K. Masuda and T. Tsuzuki, *Tetsu to Hagane*, **84**, 36 (1998).
5. Y. H. Chung, Y. H. Hwang, J. Y. Yoo, and K. Y. Kim, *Corrosion*, **58**, 479 (2002).
6. Patent, Jp. No.H07-242993 (1995).
7. K. Y. Kim, Y. H. Chung, Y. H. Hwang, and J. Y. Yoo, *Corrosion*, **58**, 570 (2002).
8. U. R. Evans and C. A. J. Taylor, *Corrosion Science*, **12**, 227 (1972).